THE JOURNAL OF BIOLOGICAL CHEMISTRY VOL. 284, NO. 45, pp. 31122–31129, November 6, 2009

Human Naa50p (Nat5/San) Displays Both Protein N^{α}- and N^{ϵ}-Acetyltransferase Activity*[S]

Received for publication, March 31, 2009, and in revised form, August 18, 2009 Published, JBC Papers in Press, September 10, 2009, DOI 10.1074/jbc.M109.001347

Rune Evjenth[‡], Kristine Hole[‡§¶], Odd A. Karlsen[‡], Mathias Ziegler[‡], Thomas Arnesen[‡§¶], and Johan R. Lillehaug[‡1]

From the Departments of [‡]Molecular Biology and [§]Surgical Sciences, University of Bergen, N-5020 Bergen, Norway and the [¶]Department of Surgery, Haukeland University Hospital, N-5021 Bergen, Norway

Protein acetylation is a widespread modification that is mediated by site-selective acetyltransferases. KATs (lysine N^{ϵ}-acetyltransferases), modify the side chain of specific lysines on histones and other proteins, a central process in regulating gene expression. N^{α}-terminal acetylation occurs on the ribosome where the α amino group of nascent polypeptides is acetylated by NATs (N-terminal acetyltransferase). In yeast, three different NAT complexes were identified NatA, NatB, and NatC. NatA is composed of two main subunits, the catalytic subunit Naa10p (Ard1p) and Naa15p (Nat1p). Naa50p (Nat5) is physically associated with NatA. In man, hNaa50p was shown to have acetyltransferase activity and to be important for chromosome segregation. In this study, we used purified recombinant hNaa50p and multiple oligopeptide substrates to identify and characterize an N^{α}-acetyltransferase activity of hNaa50p. As the preferred substrate this activity acetylates oligopeptides with N termini Met-Leu-Xxx-Pro. Furthermore, hNaa50p autoacetylates lysines 34, 37, and 140 *in vitro*, modulating hNaa50p substrate specificity. In addition, histone 4 was detected as a hNaa50p KAT substrate *in vitro*. Our findings thus provide the first experimental evidence of an enzyme having both KAT and NAT activities.

Protein acetylation is performed by two distinct types of enzymes, histone acetyltransferases/lysine acetyltransferases (KATs)[2] and N-terminal acetyltransferases (NATs). It is widely believed that the NAT complexes modify exclusively proteins at the N termini, whereas the KAT enzymes only lysine side chains.

KAT enzymes acetylate the ϵ-amino group of specific lysines on histone proteins as a crucial part of regulating gene expression (1). The KAT family consists of several members, but the p300 enzyme and its paralogue, CREB-binding protein (CBP), have been identified to account for most of the KAT activity (1). Dysregulation of p300/CBP activity has been implicated in several types of cancers and cardiac diseases (2).

The NAT complexes are physically associated with ribosomes and transfer the acetyl group from acetyl-CoA to the N-terminal α-amino group of newly synthesized proteins (3, 4). In yeast and humans, three different NAT complexes were identified, NatA, NatB, and NatC, whose activities were found to account for the majority of N^{α}-terminal acetylation (5).

The yeast NatA complex is composed of the catalytic subunit Naa10p (earlier known as Ard1p (6)) and the auxiliary subunit Naa15p (earlier known as Nat1p (6, 7)). The yNatA complex has a broad substrate specificity acetylating proteins with Ser, Ala, Gly, Val, Cys, or Thr N termini (8). A third subunit, Naa50p (earlier known as Nat5p (6)), was found to be physically associated with the yNatA complex, but no influence on the NatA activity was detected (4). The presence of a third subunit in the NatA complex has also been demonstrated in the fruit fly, dSan (9), and human, hNaa50p (hNat5p) (10).

Recently, human Naa50p was reported to acetylate itself and purified chromosome pellets *in vitro* (11). Loss of this protein led to chromatid cohesion defects in both the fruit fly and humans (9, 11). In addition, a recent study of Naa50p in the fruit fly demonstrated its importance in chromosome resolution and segregation (12).

HeLa cells with small interfering RNA-mediated down-regulation of h*NAA10* and h*NAA15*, showed decreased acetylation levels of several proteins matching the predicted NatA specificity (8). In addition, one protein, having an N-terminal sequence that deviated from the NatA substrate pattern, was also less acetylated in h*NAA10*/h*NAA15* knockdown cells. This protein, hnRNP F, has the N-terminal protein sequence MLGPEGG (8). It has been established that knockdown of either h*NAA10* or h*NAA15* in HeLa cells causes a reduced level of the hNaa50p protein (11). Therefore hnRNP F may represent a potential hNaa50p substrate *in vivo*.

In this study, the important issue of whether hNaa50p is a bifunctional NAT and KAT enzyme has been addressed. Based on *in vitro* activity assays and mass spectrometric analyses, it is demonstrated that hNaa50p indeed possesses both NAT and KAT activities. Autoacetylation of hNaa50p was observed in lysine residues 34, 37, and 140, and hNaa50p specifically acetylated histone 4 *in vitro*. The preferred N-terminal sequence for the NAT activity of hNaa50p matches the sequence of the hypothesized *in vivo* substrate, hnRNP F.

* This work was supported by The Norwegian Cancer Society, The Meltzer Foundation, and the Norwegian Health Region West.

[S] The on-line version of this article (available at http://www.jbc.org) contains supplemental Tables S1–S3 and Figs. S1–S3.

[1] To whom correspondence should be addressed: Thormohlensgate 55, N-5020 Bergen, Norway. Tel.: 47-55-58-64-21; Fax: 47-55-58-96-83; E-mail: Johan.lillehaug@mbi.uib.no.

[2] The abbreviations used are: KAT, lysine N^{ϵ}-acetyltransferases; NAT, N-terminal acetyltransferase; hnRNP, heterogeneous nuclear ribonucleoprotein; MS, mass spectrometry; V/K, V_{max}/K_m; acLys, acetylated lysine; CBP, CREB-binding protein; CREB, cAMP-response element-binding protein; HPLC, high pressure liquid chromatography; MALDI-TOF, matrix-assisted laser desorption ionization time-of-flight; GST, glutathione *S*-transferase; WT, wild type.

EXPERIMENTAL PROCEDURES

Xpress-hNaa50p Immunoprecipitation and in Vitro Acetyltransferase Assay—Overexpression and immunoprecipitation of Xpress-hNaa50p were done as described (13). The acetyltransferase assay used to test the Xp-hNaa50p activity and the initial peptide screen were performed as described previously (13). The enzyme was incubated in 250 μl of KAT buffer (50 mM Tris-HCl (pH 8.5), 10% glycerol, 1 mM EDTA) with 5 μl of [1-^{14}C]acetyl-CoA (56 mCi/mmol, GE Healthcare) and 2.5 μl of custom made peptide (2 mM; Biogenes) as substrates. After a 2-h incubation at 37 °C, the peptides were isolated using SP-Sepharose resin (Sigma). Incorporation of acetyl groups was determined by scintillation counting. Because the first residues of the peptide seemed to be most important for enzyme specificity (5), all peptides used in this study vary only within the 7 first N-terminal positions. The next 17 amino acids, indicated by "RRR," are identical for all peptides and resemble the sequence of adrenocorticotropic hormone (ACTH), except, all Lys residues have been replaced by Arg to minimize the potential interference by N^{ϵ}-acetylation. The positively charged Arg residues facilitate peptide solubility and effective isolation by cation exchange Sepharose beads. See supplemental Table S1 for peptide sequence information.

Plasmid Construction, Protein Expression, and Purification—Prokaryotic expression and purification of recombinant protein was conducted as described (14). The cDNA encoding hNaa50p was cloned into pETM-glutathione *S*-transferase (GST) (G. Stier, EMBL, Germany) for expression in *Escherichia coli*. The plasmid encoding Xpress-tagged hNaa50p was previously described (10).

Determination of Steady-state Kinetic Constants by Reverse Phase HPLC—The enzyme activity of hNaa50p was determined by reverse phase HPLC as described (15). Elution times of unmodified peptides were established by injecting pure unmodified peptide on the HPLC system, collecting fractions that corresponded to the absorbance peak of the peptide, and verification of the mass by mass spectrometry (see Fig. 4*A*). Kinetic parameters were calculated by nonlinear regression analysis using the SigmaPlot Technical Graphing Software (SPSS Inc.).

Mass Spectrometric Verification of Acetylation—Elution times of acetylated peptides were determined by collecting fractions of corresponding absorbance peaks and verifying the molecular mass by MS. The MS data showed increased molecular masses of ~42 Da, consistent with the acetylation of one residue. Prior to the MS analyses, the samples were diluted 1:1 with a matrix solution consisting of 8 μg/μl alfa-cyano-4-hydroxycinnamic acid, 60% acetonitrile, 15% methanol, and 0.1% trifluoroacetic acid. 1 μl of the sample/matrix mixtures was placed on the target plate (Bruker Daltonics, MTP 384 polished steel). The MALDI-TOF MS analyses were performed with an Ultraflex mass spectrometer (Bruker Daltronics) in a positive-ion mode. Peptide calibration standard (Bruker Daltonics) was mixed 1:1 with matrix solution and placed on the target along with the samples and used for external calibration.

Xpress-hNaa50p and purified GST-hNaa50p separated by SDS-PAGE were excised from gels and washed twice in 50 mM ammonium bicarbonate and 50% acetonitrile. Prior to protease treatment the washed gel pieces were dehydrated by vacuum centrifugation and subsequently treated with dithiothreitol and iodoacetamide for reduction and alkylation of cysteines as described (16). "In gel" digestion with Lys-C endoproteinase was carried out essentially as described by the manufacturer (Roche Applied Science). The digested peptides were purified and concentrated as described (17), and MALDI-TOF MS and MS/MS analyses were performed with an Ultraflex mass spectrometer (Bruker Daltronics) and a matrix solution consisting of 8 μg/μl alfa-cyano-4-hydroxycinnamic acid, 60% acetonitrile, 15% methanol, and 0.1% trifluoroacetic acid.

Generation of GST-hNaa50p Mutants—Mutagenesis was performed as recommended by Stratagene. See supplemental data for primer sequences. The identities of GST-hNaa50p mutants were verified by DNA sequencing.

In Vitro N^{ϵ}-Acetylation Assays—22.5 μl of purified hNaa50p (0.8 mg/ml) was mixed with 37.5 μl of [1-^{14}C]acetyl-CoA (56 mCi/mmol, GE Healthcare) and 262.5 μl of KAT buffer. The mixture was distributed into 2 tubes. One tube was incubated at 37 °C, and aliquots were collected after 0, 30, 60, 90, and 120 min. The other tube was incubated at 4 °C, and an aliquot was collected after 120 min. The enzyme activity was quenched by adding SDS-PAGE sample buffer.

For kinetic analyses of the autoacetylation reaction, 5 μM GST-hNaa50p was incubated with 500 μM acetyl-CoA containing [1-^{14}C]acetyl-CoA and KAT buffer at 37 °C. Aliquots were collected at six different time points and the enzyme reaction stopped by cooling and adding trifluoroacetic acid to a final concentration of 1% (v/v). Autoacetylated GST-hNaa50p was isolated by reverse phase HPLC and analyzed by scintillation counting.

Autoacetylation of GST-hNaa50p WT, or its R84A and Y124F mutants was performed adding 10 μl of the purified GST fusion protein (11 μM) to 30 μl of KAT buffer and 5 μl of non-radioactive acetyl-CoA (5 mM). The samples were incubated at 37 °C for 1 h, and the activity quenched by adding SDS-PAGE sample buffer. Acetylation was detected by Western blotting using an anti-acLys antibody (Upstate). The NAT assay was performed in the presence of 100 μM acetyl-CoA, 30 μM ^{1}MLGP-RRR^{24} peptide, and 50 nM of each enzyme in KAT buffer. The samples were incubated at 37 °C for 30 min prior to adding trifluoroacetic acid to 1% (v/v). The resulting acetylation was analyzed using reverse phase HPLC as described above.

For autoacetylation assays with GST-hNaa50p WT and the different lysine mutants, 2.4 μM protein was mixed with 500 μM acetyl-CoA in the above mentioned KAT buffer. The samples were incubated at 37 °C for 1 h, and the activity quenched by adding SDS-PAGE sample buffer. Acetylation was detected by Western blotting using an anti-acLys antibody (Upstate).

To explore the effect of autoacetylation on the NAT activity of hNaa50p, 10 μM purified GST-hNaa50p was incubated at 37 °C for 120 h with either 300 μM acetyl-CoA or H_2O as control in KAT buffer. An extensive incubation was chosen to ensure a high yield of autoacetylation. To determine K_m values for ^{1}MLGP-RRR^{24} or ^{1}MIGP-RRR^{24} using these enzyme variants, 30 nM autoacetylated GST-hNaa50p was incubated with either ^{1}MLGP-RRR^{24} (20–400 μM) or ^{1}MIGP-RRR^{24} (50–500

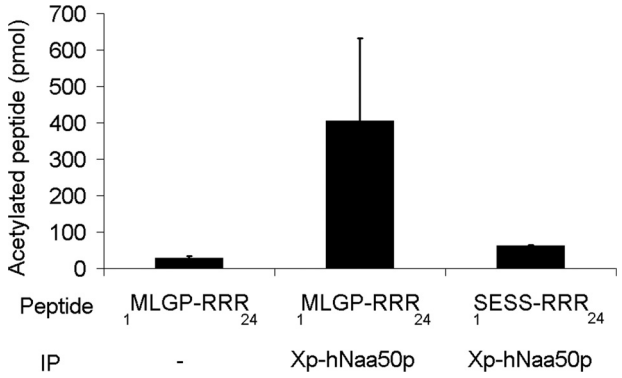

FIGURE 1. ***In vitro* acetyltransferase activity of immunoprecipitated Xpress-hNaa50p.** Immunoprecipitated Xpress-hNaa50p from transfected human embryonic kidney 293 cells was incubated with [1-^{14}C]acetyl-CoA and the oligopeptides ^{1}MLGP-RRR^{24} or ^{1}SESS-RRR^{24} for 2 h at 37 °C. dH_2O used as negative control (−). After incubation, the oligopeptides were isolated with SP-Sepharose beads, washed three times with 0.5 M acetic acid, and analyzed with scintillation counting. *Error bars* (S.D.) are based on three independent experiments. For details see "Experimental Procedures."

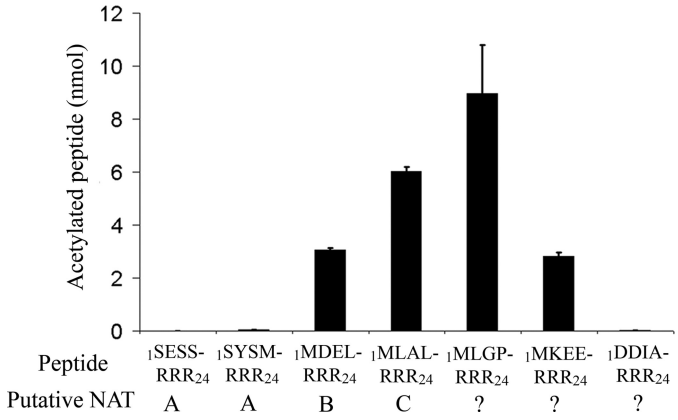

FIGURE 2. **hNaa50p/hSan acetylation of peptides with the N termini Met-Leu or Met-Asp.** Purified GST-hNaa50p was incubated with selected oligopeptides and [1-^{14}C]acetyl-CoA for 2 h at 37 °C. After incubation, the oligopeptides were isolated with SP-Sepharose beads, washed three times with 0.5 M acetic acid, and analyzed with scintillation counting. Activity detected in the negative control (dH_2O) was subtracted. The NAT complexes that are expected to perform the acetylation *in vivo* are given. *Error bars* (S.D.) are based on three independent experiments. For details see "Experimental Procedures."

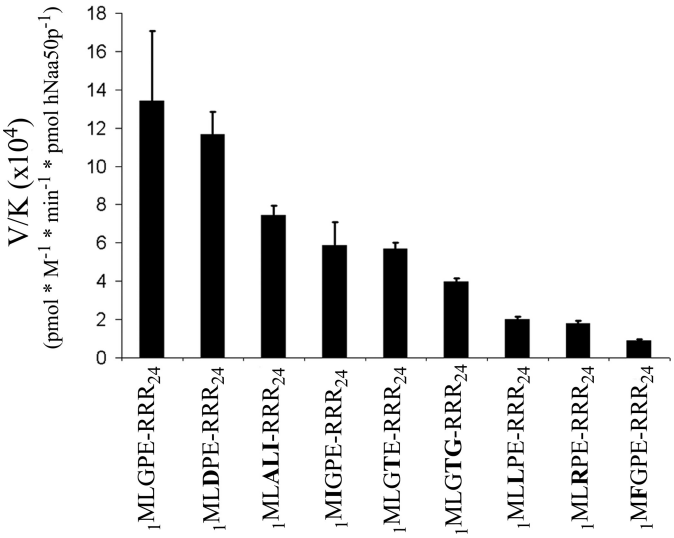

FIGURE 3. **GST-hNaa50p specificity constants (V/K).** 70 nM GST-hNaa50p was incubated with selected oligopeptide substrates for 30 min at 37 °C with saturated levels of acetyl-CoA (300 μM). The acetylation kinetics were determined with reverse phase HPLC. *V/K* is the V_{max}/K_m (oligopeptides). *Error bars* indicate the S.D. Experiments were performed in triplicate. For details see "Experimental Procedures."

RESULTS

hNaa50p Exhibits Preferred NAT Activity on Substrates Sharing the N Terminus with hnRNP F—In vitro acetyltransferase assays were performed using immunoprecipitated Xp-hNaa50p from human embryonic kidney 293 cells. Xp-hNaa50p did not extensively acetylate a ^{1}SESS-RRR^{24} oligopeptide, a known hNatA substrate (8), whereas the ^{1}MLGP-RRR^{24} oligopeptide was readily acetylated (Fig. 1). This experiment indicates that hNaa50p expressed in cell cultures has N^{α}-acetyltransferase activity toward an oligopeptide whose N terminus is identical to that of the hnRNP F protein.

Recombinant hNaa50p Preferentially Acetylates the N Termini of Met-Leu Oligopeptides—To establish the substrate specificity of hNaa50p in comparison to known NAT complexes, oligopeptides with N termini matching known NatA, NatB, and NatC substrates were tested. The putative hNaa50p substrate ^{1}MLGP-RRR^{24} and two peptides known to be N^{α}-acetylated *in vivo*, but by unknown enzymes (8), were also included. For these experiments, hNaa50p N-terminal fused to GST was expressed in *E. coli*. The purified enzyme most efficiently acetylated oligopeptides with Met-Leu N termini corresponding to putative substrates of hNatC and hNaa50p (18) (Fig. 2). The NatA substrates, ^{1}SESS-RRR^{24} and ^{1}SYSM-RRR^{24}, were not acetylated (Fig. 2).

To characterize the enzyme specificity in more detail, several additional oligopeptides with different N termini were tested (Fig. 3 and Tables 1 and 2). The calculating specificity constants (V/K), show that hNaa50p has high specificity toward oligopeptides starting with ML and with a relatively small residue in the third position. Peptides with the N-terminal sequence MD and

TABLE 1
Preferred substrates of hNaa50p-mediated acetylation

Substrates	K_m	k_{cat}
	μM	min^{-1}
Acetyl-CoA[a]	6.9 ± 0.7[b]	
^{1}MLGP-RRR^{24}	79 ± 6[b]	7.2 ± 0.7[b]

[a] The kinetic parameters for acetyl-CoA were determined in triplicate in the presence of the ^{1}MLGP-RRR^{24} peptide (150 μM). The other values were determined in duplicate or triplicate with ± S.D. For experimental details, see "Experimental Procedures" and supplemental data.

[b] Experiments were performed in duplicate or triplicate. The recorded values are average ± S.D.

MK were not acetylated at detectable levels (Table 2). Interestingly, the ^{1}MLGP-RRR^{24} (representing hnRNP F) and ^{1}MLDP-RRR^{24} (^{1}MLGP-RRR^{24} G3D) peptides were the best substrates. Table 1 shows kinetic parameters obtained for acetyl-CoA and the best *in vitro* oligopeptide substrate found so far, ^{1}MLGP-RRR^{24}. The K_m for acetyl-CoA was estimated to be 6.9 μM, whereas the K_m for the ^{1}MLGP-RRR^{24} peptide was determined to be ~75 μM with a k_{cat} of 7 min^{-1}.

TABLE 2

hNaa50p steady-state kinetic parameters for tested oligopeptide substrates

Experiments were performed in duplicate or triplicate. The recorded values are average ± S.D. The steady-state kinetic constants for the oligopeptides were determined in the presence of 300 μM acetyl-CoA. For more experimental details, see "Experimental Procedures" and supplemental data.

Peptide substrates (N terminus)	K_m	k_{cat}
	μM	min^{-1}
^{1}MLGPE-RRR^{24}	79 ± 6	7.2 ± 0.7
^{1}MLDPE-RRR^{24}	91 ± 12	7.2 ± 1.6
^{1}MIGPE-RRR^{24}	185 ± 20	10.9 ± 3[a]
^{1}MLALI-RRR^{24}	190 ± 70	6.8 ± 0.4
^{1}MLGTG-RRR^{24}	320 ± 20	2.3 ± 0.2
^{1}MLGTE-RRR^{24}	416 ± 185	5.6 ± 0.1
^{1}MLRPE-RRR^{24}	460 ± 94	—[b]
^{1}MLLPE-RRR^{24}	478 ± 305	—[b]
^{1}MFGPE-RRR^{24}	3734 ± 815	—[b]
^{1}MKEEV-RRR^{24}	—[c]	—[c]
^{1}MDELF-RRR^{24}	—[c]	—[c]

[a] V_{max} value (picomole of acetylated peptide min^{-1} pmol of hNaa50p^{-1}) is given.
[b] Due to high K_m values for these oligopeptide, it was not possible to determine k_{cat} at [peptide] $\gg K_m$.
[c] These oligopeptides were tested as substrates, but were not acetylated to a detectable level under our assay conditions.

To verify that the observed modification catalyzed by hNaa50p was indeed the transfer of an acetyl group to the peptide N terminus, modified and unmodified ^{1}MLAL-RRR^{24} peptides were separated by reverse phase HPLC and analyzed by MALDI-TOF mass spectrometry (Fig. 4*A*). The resulting MS profiles of non-acetylated ^{1}MLAL-RRR^{24} peptide (*upper panel*) revealed a MALDI molecular ion of *m*/*z* 2947.68, which is consistent with the theoretical molecular mass of the peptide (2947.7 Da). Acetylation of the ^{1}MLAL-RRR^{24} peptide (*lower panel*) should increase its molecular mass by 42 Da. Indeed a MALDI molecular ion of *m*/*z* 2990.12 was detected in the MS analyses (Fig. 4*A*).

Chemically N-terminal-acetylated ^{1}MLGP-RRR^{24} peptide was then used as substrate in the hNaa50p acetylation assay to test whether additional acetylation could occur. The N-terminal acetylated ^{1}MLGP-RRR^{24} (Ac-^{1}MLGP-RRR^{24}) peptide was not further acetylated as shown in Fig. 4*B*. These data further suggest that hNaa50p is an authentic NAT acetylating proteins at their N termini.

Autoacetylation of hNaa50p at Lysine 34, 37, and 140 in Vitro and Detection of Acetylated Lysine 34 and 140 in Vivo—hNaa50p was earlier reported to perform autoacetylation, indicative of an N^{ϵ}-acetyltransferase activity (11). To study if hNaa50p is acetylated *in vivo*, Xp-hNaa50p expressed in HeLa cells was isolated and analyzed by mass spectrometry. Two peptides in the mass spectrometry spectra showed *m*/*z* ratios at 2173.19 and 1987.08, corresponding to acetylated Lys^{34} (supplemental Fig. S1*A*) and Lys^{140} (supplemental Fig. S1*B*), respectively. This acetylation could indicate that hNaa50p is a substrate for an unknown KAT, or that it acetylates itself. To test the possibility of autoacetylation, hNaa50p from an *E. coli* extract was purified and incubated with [1-^{14}C]acetyl-CoA at 37 or 4 °C. Incubation at 37 °C showed a time-dependent increase in radioactively labeled protein, whereas the hNaa50p protein being incubated at 4 °C had no detectable level of acetylation (Fig. 5*A*). To quantify the autoacetylation reaction, purified GST-hNaa50p was incubated with [1-^{14}C]acetyl-CoA at 37 °C, and aliquots were collected at 6 different time points. GST-hNaa50p was isolated by reverse phase HPLC and the extent of modification determined by scintillation counting (Fig. 5*B*). Given that 150 pmol of GST-

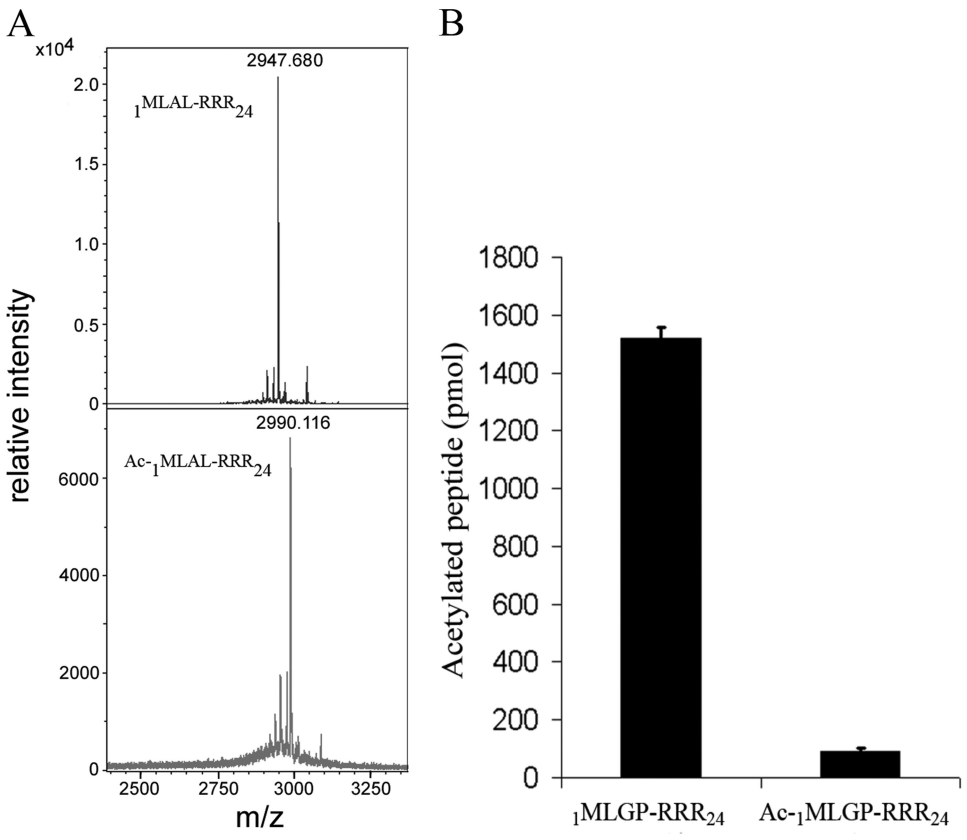

FIGURE 4. **Verification of hNaa50p N^{α}-acetyltransferase activity.** *A*, MALDI-MS spectra (mass range 2.400–3.350) of non-acetylated (*upper panel*), and acetylated ^{1}MLAL-RRR^{24} peptide (*lower panel*) after *in vitro* acetylation with GST-hNaa50p. Monoisotopic peaks are labeled with their respective *m*/*z* ratios. *B*, purified GST-hNaa50p was incubated for 2 h at 37 °C with ^{1}MLGP-RRR^{24} peptide and a chemically N-terminal acetylated version of the ^{1}MLGP-RRR^{24} peptide (Ac-^{1}MLGP-RRR^{24}). After incubation, the oligopeptides were isolated with SP-Sepharose beads, washed three times in 0.5 M acetic acid, and analyzed with scintillation counting. *Error bars* (S.D.) are based on three independent experiments.

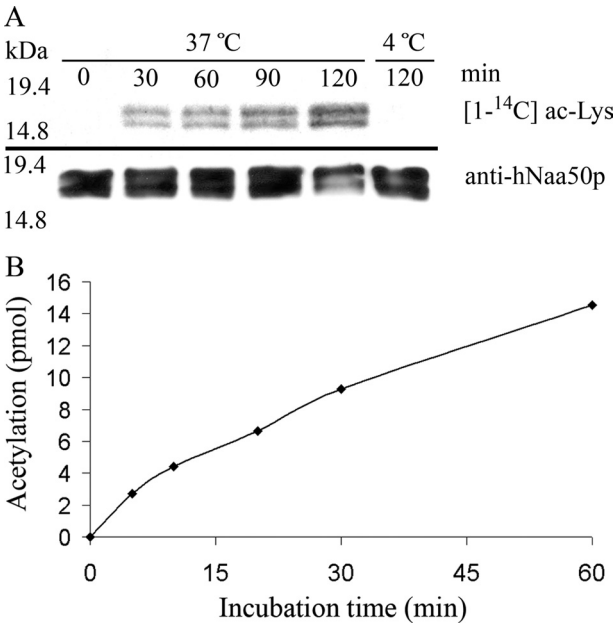

FIGURE 5. **The *in vitro* autoacetyltransferase activity of purified wild type hNaa50p.** *A,* purified hNaa50p was incubated with [1-^{14}C]acetyl-CoA for the indicated times and analyzed by autoradiography and Western blotting with anti-hNaa50p antibody. *Upper panel* indicates the increased level of [1-^{14}C]acetyl incorporation as a response to increased incubation time at 37 °C. No acetylation is detectable in the sample incubated for 120 min at 4 °C. *Lower panel* represents Western blot analyses with anti-hNaa50p showing an equal amount of hNaa50p present in the assay. *B,* purified GST-hNaa50p (3 μM) was incubated with acetyl-CoA (500 μM with 33% radioactive acetyl-CoA) at 37 °C, and samples were collected at 6 different time points. After isolating the oligopeptides with reverse phase HPLC, the acetylation was quantified by scintillation counting of incorporated radioactivity.

hNaa50p incorporated 2.7 pmol of acetyl groups over a time period of 5 min, this assay suggests an enzyme turnover that is almost 2000 times slower than the highest recorded value for the acetylation of NAT substrate (Table 2).

Because the autoacetylation assay does not discriminate between N$^{\alpha}$-terminal acetylation and N^{ϵ}-acetylation, the site(s) of modification were identified. GST-hNaa50p was autoacetylated for 60 min and analyzed by mass spectrometry. Moreover, the protein was digested with the Lys-C endoprotease, which is unable to cleave C-terminal acetylated lysines (19). The mass spectrometry analyses of the resulting peptides revealed three MALDI molecular ions of *m*/*z* 1552.769, 1986.980, and 2173.072, corresponding to predicted peptides with a 42-Da increase compared with their theoretical molecular masses (supplemental Fig. S2). An acetylated internal lysine was verified in all peptides by MS/MS analyses and established *y*- and *b*-ion series covering the acetylated lysine residues (supplemental Fig. S2, *B–D*). In addition, a specific acetyllysine marker ion at *m*/*z* 126 was detected in all MALDI MS/MS experiments further confirming that an acetylated lysine is present in the peptides (19). Sequence mapping of hNaa50p using the MS results identified lysines 34 and 140 as acetylated, the same residues as detected *in vivo*. In addition, lysine 37 was also observed as acetylated *in vitro*.

In KAT assays, a significant amount of acetyl-CoA spontaneously reacts with substrate lysines (20), a reaction that can lead to a false-positive interpretation of the acetylation assays. To verify that the observed autoacetylation of hNaa50p was due to enzymatic activity and not a chemical acetylation, we attempted to generate mutants of hNaa50p that were expected to have reduced enzyme activity. Alignment of the amino acid sequence of hNaa50p with proteins in the GCN5 family from yeast, *Tetrahymena,* and human, show that Arg^{84} of hNaa50p is central in the acetyl-CoA binding motif ^{84}**R**RL**G**I**G** (Fig. 6*A*). The same alignment indicated that Tyr^{124} is positioned in Motif B, which is a region of the GCN5 superfamily that was predicted to be essential for catalytic activity (11, 21). Therefore, a mutant hNaa50p was generated in which Arg^{84} was substituted by Ala, and Tyr^{124} was replaced by Phe. In a NAT assay, using ^{1}MLGP-RRR^{24} as oligopeptide substrate, more than 80% of the activity was lost for the R84A mutant, whereas the Y124F mutant had ~90% less activity than the wild type enzyme (Fig. 6*B*). Although both mutants still contained the three lysine residues identified as autoacetylation targets, a clear decrease in the acetylation signal was observed (Fig. 6*C*). Therefore,

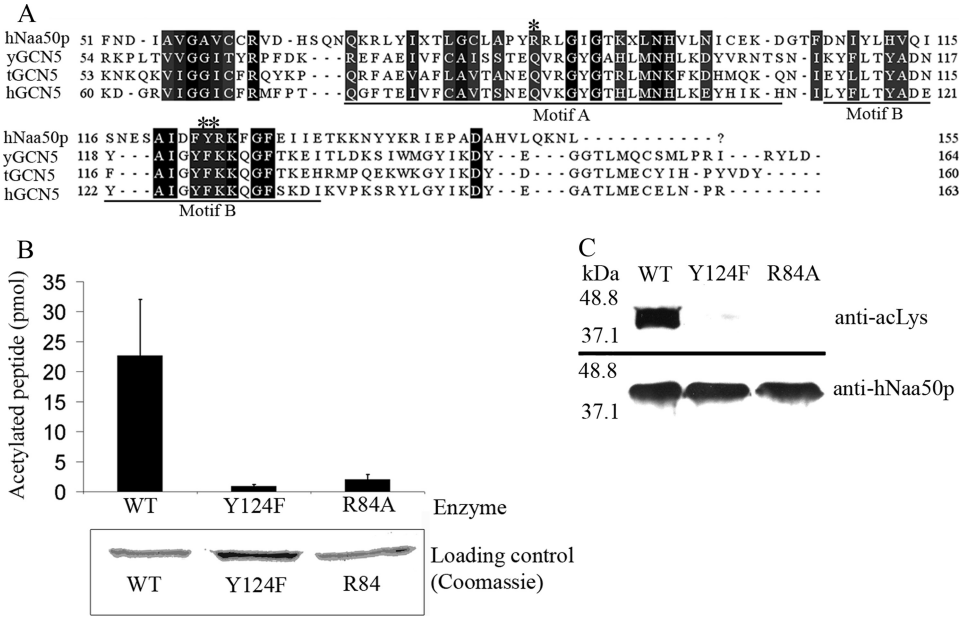

FIGURE 6. **Enzymatic activity of hNaa50p Arg^{84} to Ala or Tyr^{124} to Phe mutants.** *A,* alignment of amino acid sequences of hNaa50p with GCN5 from *Saccharomyces cerevisiae* (*yGCN5*), *Tetrahymena* (*tGCN5*), and human (*hGCN5*). The alignment indicates that Arg^{84} (*) and Tyr^{124} (**) are located in Motif A and Motif B, respectively, of the GCN5 protein fold. *B, in vitro* acetyltransferase assay comparing the enzyme activity of purified GST-hNat5 WT with GST-hNat5 Arg^{84} to Ala mutant (*R84A*) and GST-hNat5 Tyr^{124} to Phe mutant (*Y124F*). The ^{1}MLGP-RRR^{24} oligopeptide (30 μM) was used as substrate. *Error bars* (S.D.) are based on three independent experiments. Coomassie-stained SDS-PAGE verifying an equal amount of each enzyme. *C,* purified GST-hNaa50p WT and mutants were incubated for 1 h 37 °C with acetyl-CoA. Western blot analyses using anti-acetylated lysine (*anti-acLys*) antibody showed a significant difference in the autoacetylation pattern between the WT and mutants. An equal protein amount is shown by Western blotting using anti-hNaa50p.

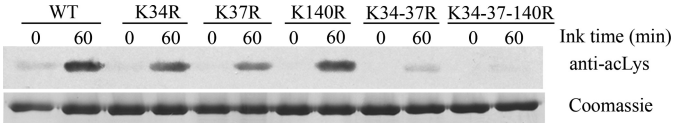

FIGURE 7. **Comparison of the autoacetylation pattern for GST-hNaa50p WT and different lysine mutants.** *Upper panel*, Western blotting analyses of GST-hNaa50p WT and different lysine to arginine mutants using anti-acetylated lysine (*anti-acLys*) antibody. 2.4 μM enzymes were incubated for 1 h at 37 °C with 500 μM acetyl-CoA. *Lower panel*, Coomassie-stained SDS-PAGE presenting protein loading.

the contribution of non-enzymatic acetylation in the KAT assays presented is negligible. Collectively these data indicate that hNaa50p is acetylated *in vivo* and that it can perform autoacetylation *in vitro* in the same residues, consistent with a possible *in vivo* autoacetylation.

The observed autoacetylation pattern was further supported using mutants of GST-hNaa50p in which Lys residues 34, 37, or 140 were replaced by Arg. In addition, a double mutant, hNaa50p K34R/K37R, and a triple mutant hNaa50p K34R/K37R/K140R were made. KAT assays with GST-hNaa50p WT and these mutants showed significantly reduced acetylation for the mutants, confirming the identification of these three Lys residues as the major targets for hNaa50p autoacetylation (Fig. 7).

The potential effect of autoacetylation on NAT activity was explored by determining the kinetic constants for the best *in vitro* substrate ^{1}M**L**GP-RRR^{24} and ^{1}M**I**GP-RRR^{24} using pre-autoacetylated and non-preautoacetylated GST-hNaa50p. These assays show that autoacetylation leads to an increase in the enzyme specificity for both oligopeptide substrates (Fig. 8). The autoacetylation led to a 2-fold decrease of the K_m values and a doubling of the maximal reaction rate (Table 3).

It was also investigated whether the KAT activity of hNaa50p might be directed toward other proteins. Several proteins known to be KAT modified *in vivo* were tested. No modification was observed when using GST-p53, GST-ODD (Oxygen dependent degradation domain within hypoxia-inducible factor-1α), or human rhSP1 (transcription factor specificity protein 1 (22)) as substrates (data not shown). However, hNaa50p KAT activity was detectable when using histone 4 as substrate. As shown in Fig. 9, a time-dependent acetylation of histone 4 was observed, as detected by anti-acLys antibodies, but only for the non-preautoacetylated GST-hNaa50p variant (Fig. 9). As negative control, GST-hNaa50p was replaced with an equal concentration of bovine serum albumin.

Potential Structural Basis for the Dual Activity of hNaa50p—To find some indications of how hNaa50p can perform both NAT and KAT functions, a structural superimposition of hNaa50p (Protein data bank code 2OB0) on a known NAT enzyme from *Salmonella typhimurium* RimL (PDB code 1S7N), and a known KAT enzyme, GNAT from *Bacillus cereus* (PDB code 3BLN) was performed (Fig. 10). All three structures were also superimposed on a KAT from *Tetrahymena* (PDB code 1PU9) that had been co-crystallized with a 19-residue oligopeptide of the H3 substrate (residue 5–23). The purpose of this structural comparison was to get an indication of how the N^{ϵ}-substrate could interact with hNaa50p (Fig. 10).

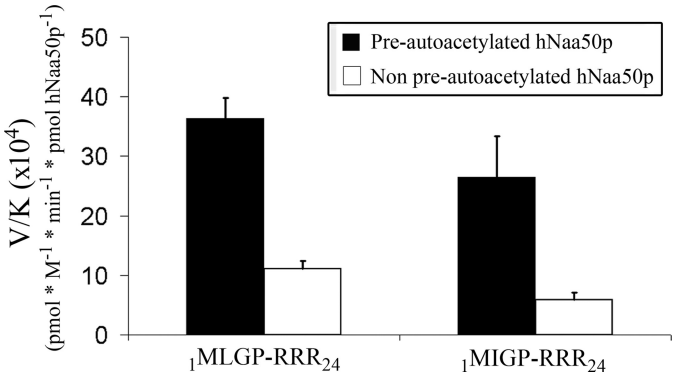

FIGURE 8. **The specificity constants (V/K) for two selected *in vitro* oligopeptide substrates using preautoacetylated and non-preautoacetylated GST-hNaa50p.** 10 μM purified GST-hNaa50p was incubated for 5 days at 37 °C with either 300 μM acetyl-CoA (*Pre-autoacetylated*) or H_2O (*Non pre-autoacetylated*). The K_m values for ^{1}MLGP-RRR^{24} or ^{1}MIGP-RRR^{24} were then determined with these enzyme variants. 30 nM GST-hNaa50p were incubated with either ^{1}MLGP-RRR^{24} (20–400 μM) or ^{1}MIGP-RRR^{24} (50–500 μM) oligopeptide substrate at 37 °C for 30 min with saturated levels of acetyl-CoA (300 μM). The acetylation kinetics were determined with reverse phase HPLC. *V/K* is the V_{max}/K_m (oligopeptides). *Error bars* indicate the S.D. Experiments were performed in triplicates.

The analyses showed that hNaa50p shares some of the flexible structural elements with GCN5. They both have loops in the entry of the substrate binding cleft (Fig. 10, *A* and *C*). In contrast, the corresponding area of RimL is composed of an antiparallel β-sheet on one side of the cleft and two short α-helixes on the other side (Fig. 10*B*).

DISCUSSION

Proteomic analyses of HeLa cell lysates, where the NatA complex was knocked down with small interfering RNAs, demonstrated reduced acetylation levels of a protein with an N-terminal sequence that did not fit with the expected hNatA substrate specificity (8). Based on the N-terminal sequence (^{1}MLGPEGG^{7}), the protein was identified to be hnRNP F, a protein that is known to interact with members of the nuclear cap-binding complex (23). Because knockdown of the human NatA complex causes reduced levels of the physical interactor hNaa50p (11) (supplemental Fig. S3), it is reasonable to speculate that the reduction of hnRNP F acetylation could be explained by a reduced amount of hNaa50p. Immunoprecipitated hNaa50p did indeed acetylate ^{1}MLGP-RRR^{24}, whereas only very low activity was observed using the NatA substrate ^{1}SESS-RRR^{24} (Fig. 1). The latter also excluded the potential presence of the catalytical subunit of NatA (hNaa10p) in the precipitates.

Kinetic experiments show that NAT substrates with the third residue small and hydrophobic, ^{1}ML**G**P-RRR^{24}, or negatively charged, ^{1}ML**D**P-RRR^{24}, function equally well as substrates. If the third position is positively charged as in ^{1}ML**R**P-RRR^{24}, acetylation is more than 5-fold reduced, based on the V/K constant (Fig. 3). Also, Leu in the third position, ^{1}ML**L**P-RRR^{24}, is suboptimal for enzyme activity. Interestingly, Pro in the fourth position, ^{1}MLG**P**-RRR^{24}, is preferred in the hNaa50p substrates, because the V/K constant of the ^{1}MLG**T**E-RRR^{24} peptide decreased by a factor of 2 (Fig. 3). The change from Pro to Thr has a minor effect on the k_{cat}, but the K_m is more than 4-fold increased (Table 2), indicating a weakened enzyme-substrate interaction. In contrast, the presence of Pro in position 2 is

TABLE 3

Effect of autoacetylation on kinetic constants

Experiments were performed in duplicate or triplicate. The recorded values are average ± S.D. For more experimental details, see "Experimental Procedures" and supplemental data.

	Non pre-autoacetylated hNaa50p		Pre-autoacetylated hNaa50p	
	K_m	V_{max} [a]	K_m	V_{max} [a]
	μM		μM	
^{1}MLGP-RRR^{24}	62 ± 10	7 ± 1.5	33 ± 5.5	12 ± 3
^{1}MIGP-RRR^{24}	186 ± 37	10.9 ± 3	80 ± 8.3	20.7 ± 3.6

[a] V_{max} is given in picomole of acetylated peptide min^{-1} pmol of hNaa50p^{-1}.

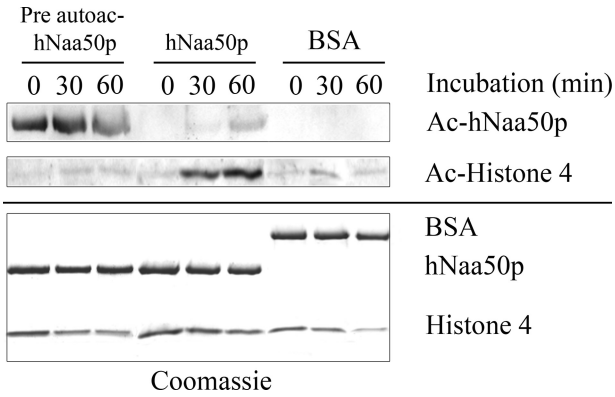

FIGURE 9. **GST-hNaa50p KAT activity on histone 4.** 10 μM purified GST-hNaa50p was incubated for 5 days at 37 °C with either 300 μM acetyl-CoA (*Pre-autoacetylated*) or H_2O (*Non pre-autoacetylated*). 2 μM of these enzyme variants were then tested for KAT activity toward Histone 4 protein (2 μM). Equal amounts of bovine serum albumin (*BSA*) replaced hNaa50p in the negative control. The samples were incubated at 37 °C, and aliquots were collected as indicated. *Upper panel*, Western blotting analyses of GST-hNaa50ps KAT activity using anti-acetylated lysine (*anti-acLys*) antibody. *Lower panel*, Coomassie-stained SDS-PAGE presenting the protein loading.

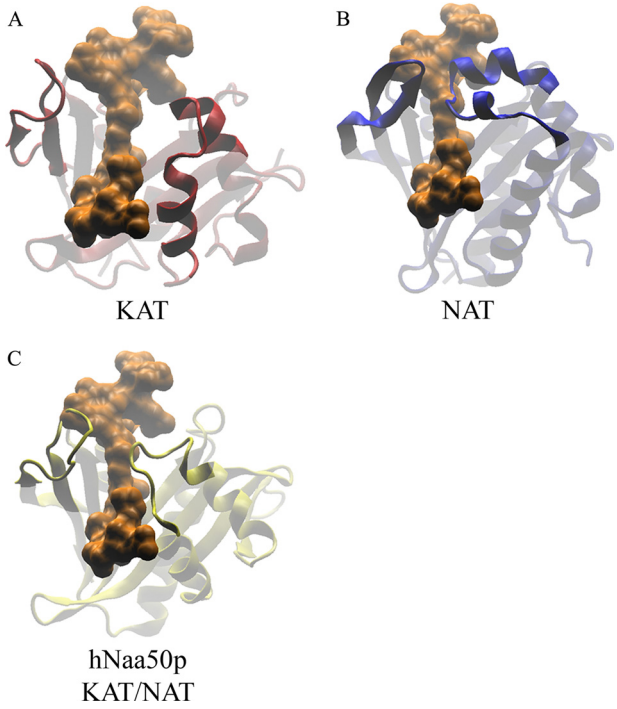

FIGURE 10. **Structural superimposing of hNaa50p, RimL from *S. thyphimurium* (NAT), and GNAT enzyme from *B. cereus* (histone acetyltransferases).** *A*, protein structure of GNAT (*B. cereus*; PDB code 3BLN) was structurally compared with tGCN5 (*Tetrahymena;* PDB code 1PU9) that had been co-crystallized with a stretch of the H3 substrate (residue 5–23) shown in *orange*. *B,* protein structure of RimL (*S. thyphimurium*; PDB code 1S7N) with the same H3 substrate stretch present in *orange*. *C,* structural comparison of hNaa50p (PDB code 2OB0) with the H3 substrate stretch in *orange*. All structures are with similar orientations, and parts the protein structures are indicated as partly transparent to clarify the point.

associated with reduced N-terminal acetylation by the NatA complex (5, 8).

The specificity of hNaa50p appears relatively similar to the specificity of the yeast NatC complex. In yeast, NatC acetylate peptides with N termini ML, MF, and MW (5). In contrast to yNatC, Phe in the second position leads to a dramatic increase in the K_m value (Table 2). Recent findings on the human NatC complex suggest that hNaa30p (hMak3, the catalytic subunit of hNatC) has a conserved substrate specificity from yeast (18). *In vitro* acetylation assays showed that hNaa30p-acetylated oligopeptides with N-terminal sequences of ^{1}MLALI-RRR^{24}, ^{1}MLGTG-RRR^{24}, and ^{1}MLGTE-RRR^{24} are more than 2-fold better than ^{1}MLGPE-RRR^{24}. Therefore, the substrate preference regarding the ML group of peptides differs between hNaa50p and hNatC. This implies that hNaa50p and hNaa30p acetylate similar, but distinct N-terminal substrates *in vivo*, and that the hNaa50p activity is restricted to a specific subset of substrates previously assumed to be NatC substrates.

hNaa50p was earlier reported to perform autoacetylation, which most likely represents N^{ϵ}-acetylation. The results of the present study verify this supposition. Moreover, they strongly suggest that autoacetylation of hNaa50p is of physiological relevance. Lysine residues 34 and 140 were identified as acetylation target sites both when the protein was immunoprecipitated from HeLa cells or autoacetylated *in vitro*. Moreover, autoacetylation led to an increase in its NAT, but not KAT activity.

Autoacetylation of hNaa50p leads to an increased enzyme specificity as indicated by a decreased K_m value and increased enzyme activity. This appears to be a general effect as it was observed for both a highly preferred (^{1}MLGP-RRR^{24}) and suboptimal substrate (^{1}MIGP-RRR^{24}). The decrease in K_m indicates an improved enzyme-substrate interaction and autoacetylation may thus reflect a potential specificity switch *in vivo*.

Besides its autoacetylation, hNaa50p might also exert KAT activity toward other proteins. Although no such activity could be detected using GST-p53, GST-ODD, or rhSP1 as substrates, histone 4 was modified. Interestingly, whereas the NAT activity of hNaa50p was enhanced by autoacetylation, the KAT activity toward histone 4 was clearly reduced. This could indicate that autoacetylation mediates increased enzyme specificity. Further studies are required to establish whether or not histone 4 is a hNaa50p KAT substrate *in vivo*.

The observed phenotypes following silencing of Naa50p/San in *Drosophila* or human cells (9, 11) indicate that important *in vivo* substrates are involved in sister chromatid cohesion. Blastp searches in the Swiss-Prot data base (version 56.0) for human proteins that match the preferred N-terminal sequence for the NAT activity of hNaa50p resulted in several hits, including TIMELESS-interacting protein, a protein that is reportedly involved in chromatid cohesion (24, 25) (supplemental Table S3).

hNaa50p is the first acetyltransferase to be identified as having both NAT and KAT activity. Several KAT enzymes have been structurally determined, but only a few NAT structures from prokaryotic organisms were solved. Therefore it is difficult to explain the dual acetylation capacity of hNaa50p in structural terms. However, comparison of the structures provided some hints. hNaa50p is constructed with flexible loops in the entry site of the substrate binding cleft (Fig. 10*C*). This is a structural property that hNaa50p shares with the KAT enzymes (Fig. 10*A*). These loops could allow for flexibility to accommodate larger substrates, such as protein surfaces that could make a productive interaction with hNaa50p. RimL, representing the NAT enzymes, has in the corresponding area an antiparallel β-sheet on one side and two short α-helixes on the other (Fig. 10*B*). These secondary structures are expected to be more rigid and hence reduce the area of interaction possibly required for ϵ-acetylation.

In conclusion, hNaa50p displays N^{α}-acetyltransferase activity and prefers substrates that have ML at their N termini. In addition, hNaa50p has the capacity for N^{ϵ}-autoacetylation, targeting Lys^{34}, Lys^{37}, and Lys^{140}. It is thus the first identified bifunctional protein acetyltransferase exhibiting both KAT and NAT activities.

Acknowledgments—We thank E. Skjelvik, L. Vikebø, M. Algrøy, H. Halseth, and N. Glomnes for technical assistance.

REFERENCES

1. Marmorstein, R. (2004) *Methods Enzymol.* **376,** 106–119
2. Kalkhoven, E. (2004) *Biochem. Pharmacol.* **68,** 1145–1155
3. Polevoda, B., Brown, S., Cardillo, T. S., Rigby, S., and Sherman, F. (2008) *J. Cell. Biochem.* **103,** 492–508
4. Gautschi, M., Just, S., Mun, A., Ross, S., Rücknagel, P., Dubaquié, Y., Ehrenhofer-Murray, A., and Rospert, S. (2003) *Mol. Cell. Biol.* **23,** 7403–7414
5. Polevoda, B., and Sherman, F. (2003) *J. Mol. Biol.* **325,** 595–622
6. Polevoda, B., Arnesen, T., and Sherman, F. (2009) *BMC Proc.* **3,** Suppl. 6, S2
7. Park, E. C., and Szostak, J. W. (1992) *EMBO J.* **11,** 2087–2093
8. Arnesen, T., Van Damme, P., Polevoda, B., Helsens, K., Evjenth, R., Colaert, N., Varhaug, J. E., Vandekerckhove, J., Lillehaug, J. R., Sherman, F., and Gevaert, K. (2009) *Proc. Natl. Acad. Sci. U.S.A.* **106,** 8157–8162
9. Williams, B. C., Garrett-Engele, C. M., Li, Z., Williams, E. V., Rosenman, E. D., and Goldberg, M. L. (2003) *Curr. Biol.* **13,** 2025–2036
10. Arnesen, T., Anderson, D., Torsvik, J., Halseth, H. B., Varhaug, J. E., and Lillehaug, J. R. (2006) *Gene* **371,** 291–295
11. Hou, F., Chu, C. W., Kong, X., Yokomori, K., and Zou, H. (2007) *J. Cell Biol.* **177,** 587–597
12. Pimenta-Marques, A., Tostões, R., Marty, T., Barbosa, V., Lehmann, R., and Martinho, R. G. (2008) *Dev. Biol.* **323,** 197–206
13. Arnesen, T., Anderson, D., Baldersheim, C., Lanotte, M., Varhaug, J. E., and Lillehaug, J. R. (2005) *Biochem. J.* **386,** 433–443
14. Arnesen, T., Kong, X., Evjenth, R., Gromyko, D., Varhaug, J. E., Lin, Z., Sang, N., Caro, J., and Lillehaug, J. R. (2005) *FEBS Lett.* **579,** 6428–6432
15. Evjenth, R., Hole, K., Ziegler, M., and Lillehaug, J. R. (2009) *BMC Proc.* **3,** Suppl. 6, S5
16. Shevchenko, A., Wilm, M., Vorm, O., and Mann, M. (1996) *Anal. Chem.* **68,** 850–858
17. Gobom, J., Nordhoff, E., Mirgorodskaya, E., Ekman, R., and Roepstorff, P. (1999) *J. Mass Spectrom.* **34,** 105–116
18. Starheim, K. K., Gromyko, D., Evjenth, R., Ryningen, A., Varhaug, J. E., Lillehaug, J. R., and Arnesen, T. (2009) *Mol. Cell. Biol.* **29,** 3569–3581
19. Dormeyer, W., Ott, M., and Schnölzer, M. (2005) *Mol. Cell. Proteomics* **4,** 1226–1239
20. Tanner, K. G., Trievel, R. C., Kuo, M. H., Howard, R. M., Berger, S. L., Allis, C. D., Marmorstein, R., and Denu, J. M. (1999) *J. Biol. Chem.* **274,** 18157–18160
21. Trievel, R. C., Rojas, J. R., Sterner, D. E., Venkataramani, R. N., Wang, L., Zhou, J., Allis, C. D., Berger, S. L., and Marmorstein, R. (1999) *Proc. Natl. Acad. Sci. U.S.A.* **96,** 8931–8936
22. Pugh, B. F., and Tjian, R. (1990) *Cell* **61,** 1187–1197
23. Gamberi, C., Izaurralde, E., Beisel, C., and Mattaj, I. W. (1997) *Mol. Cell. Biol.* **17,** 2587–2597
24. Yoshizawa-Sugata, N., and Masai, H. (2007) *J. Biol. Chem.* **282,** 2729–2740
25. Gotter, A. L., Suppa, C., and Emanuel, B. S. (2007) *J. Mol. Biol.* **366,** 36–52